MOLECULAR AND CELLULAR BIOLOGY, May 2008, p. 3386–3400 Vol. 28, No. 10
0270-7306/08/$08.00+0 doi:10.1128/MCB.02041-07

Abnormal Sympathoadrenal Development and Systemic Hypotension in *PHD3*$^{-/-}$ Mice$^{\nabla}$

Tammie Bishop,[1]† Denis Gallagher,[2]† Alberto Pascual,[3] Craig A. Lygate,[4] Joseph P. de Bono,[4] Lynn G. Nicholls,[1] Patricia Ortega-Saenz,[3] Henrik Oster,[4] Bhathiya Wijeyekoon,[1] Andrew I. Sutherland,[1] Alexandra Grosfeld,[1] Julian Aragones,[5,6] Martin Schneider,[5,6] Katie van Geyte,[5,6] Dania Teixeira,[2] Antonio Diez-Juan,[5,6] Jose Lopez-Barneo,[3] Keith M. Channon,[4] Patrick H. Maxwell,[7] Christopher W. Pugh,[1] Alun M. Davies,[2] Peter Carmeliet,[5,6] and Peter J. Ratcliffe[1]*

The Henry Wellcome Building for Molecular Physiology, University of Oxford, Headington Campus, Roosevelt Drive, Oxford OX3 7BN, United Kingdom[1]; School of Biosciences, Cardiff University, Museum Avenue, P.O. Box 911, Cardiff CF10 3US, United Kingdom[2]; Laboratorio de Investigaciones Biomédicas, Hospital Universitario Virgen del Rocío, Universidad de Sevilla, Sevilla, Spain[3]; The Henry Wellcome Building for Genomic Medicine, University of Oxford, Headington Campus, Roosevelt Drive, Oxford OX3 7BN, United Kingdom[4]; Department for Transgene Technology and Gene Therapy, VIB, 3000 Leuven, Belgium[5]; The Center for Transgene Technology and Gene Therapy, K. U. Leuven, 3000 Leuven, Belgium[6]; and Renal Laboratory, Hammersmith Campus, Imperial College London, Du Cane Road, London W12 0NN, United Kingdom[7]

Received 13 November 2007/Returned for modification 19 December 2007/Accepted 25 February 2008

Cell culture studies have implicated the oxygen-sensitive hypoxia-inducible factor (HIF) prolyl hydroxylase PHD3 in the regulation of neuronal apoptosis. To better understand this function in vivo, we have created *PHD3*$^{-/-}$ mice and analyzed the neuronal phenotype. Reduced apoptosis in superior cervical ganglion (SCG) neurons cultured from *PHD3*$^{-/-}$ mice is associated with an increase in the number of cells in the SCG, as well as in the adrenal medulla and carotid body. Genetic analysis by intercrossing *PHD3*$^{-/-}$ mice with *HIF-1a*$^{+/-}$ and *HIF-2a*$^{+/-}$ mice demonstrated an interaction with HIF-2α but not HIF-1α, supporting the nonredundant involvement of a PHD3–HIF-2α pathway in the regulation of sympathoadrenal development. Despite the increased number of cells, the sympathoadrenal system appeared hypofunctional in *PHD3*$^{-/-}$ mice, with reduced target tissue innervation, adrenal medullary secretory capacity, sympathoadrenal responses, and systemic blood pressure. These observations suggest that the role of PHD3 in sympathoadrenal development extends beyond simple control of cell survival and organ mass, with functional PHD3 being required for proper anatomical and physiological integrity of the system. Perturbation of this interface between developmental and adaptive signaling by hypoxic, metabolic, or other stresses could have important effects on key sympathoadrenal functions, such as blood pressure regulation.

In response to low oxygen tensions, organisms mount a wide-ranging adaptive response involving many cellular and systemic processes. Activation of hypoxia-inducible factor (HIF) plays a central role in this process, inducing transcriptional targets that enhance oxygen delivery, better adapt cells to hypoxia, or modulate cell proliferation or survival pathways (reviewed in references 16 and 37). Hypoxia may, under different circumstances, either promote or protect cells from apoptosis, and HIF itself contributes to these processes both indirectly, through the defense of cellular energy supplies, and directly, via transcriptional changes in proapoptotic or prosurvival genes. However, to generate the anatomical and physiological integrity required for oxygen homeostasis in the intact organism, these adaptive responses to hypoxia must also be accurately interfaced with the developmental control of growth.

Though the nature of these adaptive-developmental connections remains poorly understood, it is of interest that the cellular oxygen sensor PHD3 (otherwise termed EGLN3 or HPH1), one of three Fe(II)-dependent dioxygenases now known to negatively regulate HIF by prolyl hydroxylation of HIF-α subunits (HIF-1α and HIF-2α) (6, 13), had been previously identified as a gene involved in developmental apoptosis of neurons (23–25, 40). Over 50% of neurons produced during development die through apoptosis before adulthood (reviewed in references 10 and 31). This process is largely regulated by neurotrophic factors that are secreted in limited amounts by target tissues such that only those neurons making appropriate connections survive. During the investigation of these phenomena, PHD3 mRNA was identified as a neuronal transcript that is induced by withdrawal of the neurotrophin nerve growth factor (NGF) (24). Further studies have demonstrated that overexpression of PHD3 in primary sympathetic neurons cultured from the developing superior cervical ganglion and in the adrenal medullary tumor cell line PC12 results in apoptosis even in the presence of saturating quantities of NGF (23, 24). This effect was not reproduced by a catalytically inactive PHD3 mutant (23), whereas hypoxia was able to suppress apoptosis in sympathetic neurons (44). Furthermore, knock-down of PHD3 by small interfering RNA in PC12 cells prevented apoptosis even in the absence of NGF (23). Taken

* Corresponding author. Mailing address: The Henry Wellcome Building for Molecular Physiology, University of Oxford, Headington Campus, Roosevelt Drive, Oxford OX3 7BN, United Kingdom. Phone: (44) 1865 287 990. Fax: (44) 1865 287 992. E-mail: pjr@well.ox.ac.uk.

† T.B. and D.G. contributed equally to this work.

$^{\nabla}$ Published ahead of print on 10 March 2008.

together, these observations in cultured cells indicate that the oxygen-sensitive catalytic activity of PHD3 has a role in the regulation of neuronal apoptosis, raising important questions about the extent of PHD3-dependent neuronal apoptosis in vivo and its role in the intact animal.

To address this, we have inactivated PHD3 (by homologous recombination in the mouse) and have analyzed the developmental and physiological effects on neuronal apoptosis. We show that PHD3-dependent modulation of NGF-dependent survival is a lineage-specific property affecting the sympathetic nervous system and that sympathetic neurons from *PHD3*$^{-/-}$, but not *PHD2*$^{+/-}$ or *PHD1*$^{-/-}$, mice manifest increased NGF-promoted neurite growth as well as enhanced survival. Increased numbers of sympathetic neurons survive to adulthood, and *PHD3*$^{-/-}$ mice have increased numbers of neurons in the superior cervical ganglia (SCG) and increased numbers of chromaffin and glomus cells in the adrenal medulla and carotid body. However, despite this increase in cell number, the sympathoadrenal system was dysfunctional in *PHD3*$^{-/-}$ mice, with reduced innervation of target organs and dysregulated responses, including reduced catecholamine secretion and reduced systemic blood pressure. The findings demonstrate a key role for PHD3 in regulating the anatomical and physiological integrity of the sympathoadrenal system.

MATERIALS AND METHODS

Targeting vector and PHD3 inactivation. For construction of the PHD3 targeting vector, the following fragments were cloned in a pPNTLox2 vector (from 5′ to 3′): a 3.4-kb BamH1 fragment located 3.1 kb upstream of exon 1 (5′ flank) and a neomycin resistance cassette in the opposite orientation, a 3.9-kb EcoR1 fragment located 1.4 kb downstream of exon 1 (3′ flank), and a thymidine kinase selection cassette (Fig. 1A). Embryonic stem (ES) cells (129 SvEv background) were electroporated with the linearized targeting vector for PHD3 as described elsewhere (39). Resistant clones were screened for homologous recombination by Southern blotting (Fig. 1B) and PCR (not shown). Correctly recombined ES cells were then aggregated with morula-stage embryos. To obtain *PHD3*$^{+/-}$ germ line offspring in a 50% Swiss/50% 129 SvEv background, chimeric male mice were intercrossed with wild-type Swiss female mice. PHD3 mRNA transcripts were quantified by RNase protection assay in embryos (Fig. 1C), using a riboprobe protecting bp 217 to 383, 5′ to 3′, of PHD3 mRNA, and real-time reverse transcription-PCR (RT-PCR) in mouse embryonic fibroblasts (Fig. 1D), using the following forward and reverse primers: 5′-TCCCACTCTTCCACCTTC-3′ and 5′-CTGTAGCCGTATTCATTGTC-3′ for glyceraldehyde-3-phosphate dehydrogenase (GAPDH); 5′-CTATGGGAAGAGCAAAGC-3′ and 5′-AGAGC AGATGATGTGGAA-3′ for PHD3, which amplify bp 1779 to 2008, a sequence distal to the deleted region, in response to normoxia or hypoxia (1% oxygen for 16 h). PHD3 protein levels were also measured by Western blotting in mouse embryonic fibroblasts with a monoclonal mouse anti-PHD3 antibody, P3-188e (1), to confirm their absence in *PHD3*$^{-/-}$ tissues.

Animals. Wild-type, *PHD3*$^{-/-}$, *PHD1*$^{-/-}$, *PHD2*$^{+/-}$, *PHD3*$^{-/-}$; *HIF-1*$\alpha^{+/-}$, and *PHD3*$^{-/-}$; *HIF-2*$\alpha^{+/-}$ and *HIF-2*$\alpha^{+/-}$ mice on a mixed Swiss/129SvEv genetic background were used in the experiments. Mice from the same litter were used for all comparisons, except for *HIF-2*$\alpha^{+/-}$ versus *PHD3*$^{-/-}$; *HIF-2*$\alpha^{+/-}$ (see Fig. 5D, below) where appropriate crosses were unlikely, by Mendelian inheritance, to produce the required genotypes within littermates. For adult mice, males of between 3 and 6 months of age were used.

Neuronal culture. SCG, dorsal root ganglia (DRG), and trigeminal ganglia (TG) were dissected from postnatal day 0 (P0) mouse pups, trypsinized in 0.05% trypsin in Hanks' balanced salt solution (Gibco) for 20 min at 37°C, and dissociated by trituration. Dissociated cultures of SCG, DRG, and TG neurons were then plated at low density (150 to 300 cells/dish) on a poly-ornithine/laminin substrate in 35-mm tissue culture dishes in defined, serum-free medium, as described previously (11). A range of concentrations (0 to 250 ng/ml) of NGF or neurotrophin 3 (NT-3; both were from R&D Systems, Minneapolis, MN) was added to support the survival of cultured neurons.

Neuronal survival was measured by counting the number of neurons in a 12- by 12-mm grid in the center of the dish both 3 and 24 h after plating (as described in reference 11). The number of neurons surviving after 24 h was expressed as a percentage of the initial number of neurons.

Total viable neuronal counts were measured by counting the number of phase-bright neurons using a Neubauer hemocytometer immediately following dissociation of neurons.

Neuritic morphology was measured by culturing neonatal SCG neurons for 24 h with 10, 0.4, or 0.08 ng/ml NGF, as described above. Caspase inhibitors (100 μM; Calbiochem) were added to cultures containing limiting levels of NGF (0.4 and 0.08 ng/ml) in order to avoid biased sampling of differentially surviving neurons. Neurons were then fluorescently labeled with the vital dye calcein-AM (Invitrogen), and images were acquired using an Axioplan Zeiss laser scanning confocal microscope. Neuritic arbors were traced using LSM510 software in order to calculate the total neurite length and the extent of arborization by Sholl analysis. For the latter, concentric, digitally generated rings, 30 μm apart, were centered on the cell soma, and the number of neurites intersecting each ring was counted (38).

Quantitative RT-PCR. Dissociated SCG, DRG, and TG neurons from wild-type P0 mouse pups were cultured overnight in 10 ng/ml NGF as described above. Neurons were then washed with defined culture medium and grown in either the presence or absence of NGF for 10 h (the time point at which PHD3 mRNA induction is maximal in the SCG [24]) before harvesting the cells for RNA. Total RNA was isolated with the RNeasy Mini extraction kit (Qiagen, Hilden, Germany) and then reverse transcribed for 1 h at 37°C with StrataScript reverse transcriptase (Stratagene). Reverse transcription reactions were amplified using the Brilliant QPCR core reagent kit (Stratagene) according to the manufacturer's protocol. The PCR was performed with the Mx3000P apparatus (Stratagene) for 45 cycles of 95°C for 30 s, 52°C (for PHD3) or 51°C (for GAPDH) for 1 min, and 72°C for 30 s. A melting curve was obtained to confirm that the Sybr green (Molecular Probes) signal corresponded to a unique and specific amplicon. Standard curves were generated for every real-time PCR run by using serial fourfold dilutions of a reverse-transcribed RNA extract from adult heart. Primers for PHD3 and GAPDH were as described above.

Histological and stereological analyses. To estimate the total tyrosine hydroxylase (TH)-positive cell number, the SCG, adrenal medulla, and carotid body from adult mice were fixed in formalin overnight and then transferred into phosphate-buffered saline (PBS) containing 30% sucrose. Twenty-μm sections were blocked for 1 h at room temperature with 10% fetal calf serum and 1 mg/ml bovine serum albumin containing 0.1% Triton X-100 in PBS and then incubated for 16 h at 4°C with a rabbit anti-TH polyclonal antibody (Pel-Freez; diluted 1:1,000 in blocking solution). The sections were washed four times in PBS-Triton before being incubated with goat anti-rabbit secondary antibody (Envision+; Dako). Stereological estimation of the number of TH-positive cells was performed on sections spaced 80 μm (SCG and adrenal medulla) or 40 μm (carotid body) throughout the organ. The number of cells was estimated by systematic random sampling using a 106,954-μm^3 optical dissector (43), excluding cells in the superficial planes of sections. The volume of each organ was estimated according to Cavalieri's principle (8). The adrenal medulla cell volume was calculated using a rotator vertical probe. Seven randomly selected TH-positive cells were measured in different sections per individual adrenal gland. Stereological measurements were performed using the CAST grid system (Olympus) with a coefficient of error of <0.09.

To detect apoptosis in the SCG from P0 mice, tissues were fixed in formalin overnight and then transferred to 70% ethanol and paraffin embedded. The terminal deoxynucleotidyltransferase-mediated dUTP-biotin nick end labeling (TUNEL) method was performed on 7-μm sections of the SCG using the ApopTag peroxidase in situ apoptosis detection kit (Chemicon International) according to the manufacturer's directions.

To assess the density of sympathetic innervation, the eyes and submandibular and pineal glands from adult mice (or P5 mice for the pineal glands) were fixed and cryoprotected as above. Fifteen-μm serial sections were blocked for 1 h at room temperature with 10% normal goat serum containing 0.1% Triton X-100 in 10 mM PBS and then incubated for 18 h at 4°C with a rabbit anti-TH polyclonal antibody (diluted 1:200 in PBS with 1% normal goat serum; Chemicon). The sections were washed three times in PBS before being incubated with goat anti-rabbit secondary antibody (Alexa-Fluor, diluted 1:500 in PBS with 1% normal goat serum; Invitrogen). The outlines of the iris and submandibular and pineal glands were traced using Adobe Photoshop 7. The total and TH-positive areas were measured using automated pixel counts, and the ratio of TH-positive area to total area was used to calculated the TH-positive density.

Pupillometry. Adult wild-type and *PHD3*$^{-/-}$ mice were dark adapted for 1 h. Subsequently, animals were removed from their home cage, immobilized by scruffing, and pupil reactions were monitored (at 0 lx followed by 150 lx of bright white light) using a commercial charge-coupled-device camcorder (DCR-

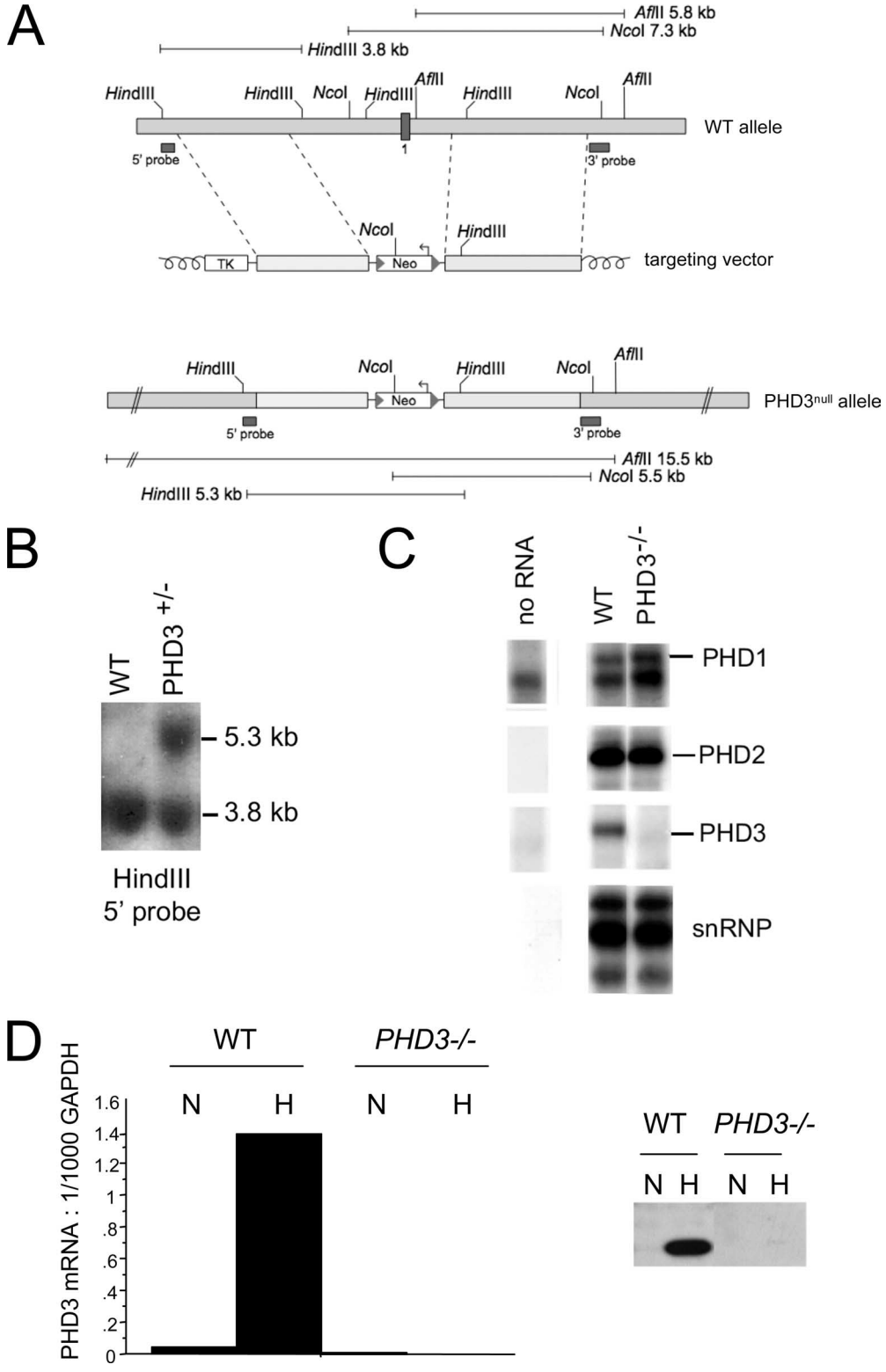

FIG. 1. PHD3 targeting strategy. (A) Targeting strategy for PHD3 inactivation. Top: wild-type PHD3 allele diagram, indicating the position of exon 1 (dark box in the genomic structure). Middle: outline of the targeting vector, specifying the genomic sequences used as 5′ and 3′ homology flanks, inserted on each side of a neomycin resistance (Neo) cassette. A thymidine kinase (TK) gene outside the flanking homologies allowed for negative selection against random integration events. Bottom: replacement of exon 1 by the Neo cassette after homologous recombination. Diagnostic restriction fragments are indicated with their relative sizes by the thin lines under or above the alleles. Dark bars under the genes represent the probes used for Southern blot analysis. (B) Southern blot analysis of genomic DNA from recombinant ES cells, digested with HindIII and hybridized with the 5′ external probe. The 3.8-kb and 5.3-kb genomic fragments correspond to PHD3 wild-type (WT) and PHD3^{null} alleles, respectively. (C) RNase protection assay demonstrating PHD1, -2, and -3 mRNA levels in total RNA extracted from wild-type and *PHD3*$^{-/-}$ embryos. U6 small nuclear RNA (snRNP) was used as an internal control. (D) Quantitative RT-PCR (left panel) and Western blot assay (right panel) showing induction of PHD3 mRNA and protein in wild-type, but not *PHD3*$^{-/-}$, mouse embryonic fibroblasts in response to hypoxia. N, normoxia; H, hypoxia (1% oxygen for 16 h).

HC17E; Sony, Tokyo, Japan) attached to a dissecting microscope (Olympus, Tokyo, Japan) under infrared light-emitting diode illumination (λ_{max} of 850 nm). Pupil areas were estimated by manually fitting an ellipse to digitalized video still images using Windows Movie Maker (Microsoft, Redmond, WA) and Adobe Photoshop (San Jose, CA) software.

In vivo hemodynamics. Adult mice were anesthetized with 2% isoflurane in 100% oxygen via a nose cone. Mice were placed supine with body temperature regulated at 37°C and allowed to breathe spontaneously. The right carotid artery was cannulated with a 1.4 French microtipped cannula (SPR-839; Millar Instruments, Houston, TX) advanced retrograde into the left ventricular (LV) cavity under ultrasound guidance. The right jugular vein was cannulated with polyethylene tubing for intravenous drug administration. Isoflurane was reduced to 1.5%, followed by a period of equilibration until hemodynamic indices were stable for >15 min. Pressure measurements were recorded using a Powerlab 4SP data recorder (ADInstruments, Chalgrove, United Kingdom) at baseline in both the LV and aorta and in the LV during infusion of β_1-adrenoreceptor stimulation with dobutamine hydrochloride (16 ng/g of body wt/min).

A subset of these mice were used to test baroreceptor reflex function by intravenous bolus administration of the α_1-adrenoreceptor agonist phenylephrine hydrochloride (at 50 μg/kg) to induce brief periods of elevated blood pressure (30). Baroreceptor reflex gain was calculated as the maximal change in heart rate over the maximal change in blood pressure. Drug solutions for bolus injection were made up in 0.9% saline and a volume of 5 μl. Mice were killed by cervical dislocation or removal of the heart, and the cardiac chambers blotted and weighed.

Radiotelemetry. PAC10 radiotelemeters (Data Sciences International, MN) were implanted in the left carotid artery of adult mice under isoflurane anesthesia as previously described (7, 29). Mice were allowed to recover for 10 days following the operation, and then continuous measurements of blood pressure and activity state were recorded, at 500 Hz, for three consecutive days using standard acquisition software (Data Sciences International, MN). Blood pressure was analyzed on a beat-per-beat basis according to the activity state of the mouse at the time of recording (Spike 2, version 6.1; Cambridge Electronic Design, Cambridge, United Kingdom). Two activity states were defined: rest, no movement of the animal as detected by the telemeter within 30 s of measurement; activity, movement of the mouse within its cage at the time of recording.

Amperometric recording of single-cell catecholamine secretion in isolated slices. Adult mouse suprarenal gland dissection, slicing, and culture, as well as the measurement of catecholamine secretion, were performed following previously described procedures (14). Slices were transferred to a recording chamber and continuously perfused with a solution containing 117 mM NaCl, 4.5 mM KCl, 23 mM $NaHCO_3$, 1 mM $MgCl_2$, 2.5 mM $CaCl_2$, 5 mM glucose, and 5 mM sucrose. When 40 mM or 20 mM potassium solutions were used, equimolar quantities of sodium were used to replace potassium. The solution was bubbled with a gas mixture of 5% CO_2 to adjust the pH to 7.2. All the experiments were performed in a chamber at 36°C. Secretion rate (femtocoulombs/min) was calculated as the amount of charge transferred to the recording electrode during a given time period (32).

Plasma catecholamines. Blood from adult mice (anesthetized with Nembutal; 600 μg/kg of body weight) was collected into heparinized tubes on ice that were then centrifuged at 6,000 × *g* for 5 min at 4°C to separate plasma. Plasma catecholamine levels were quantified by immunoassay according to the manufacturer's instructions (IBL-Hamburg).

Statistical analyses. Data are expressed as means ± standard errors of the means (SEM), with the number of experiments indicated. Statistical analyses were performed using Student's *t* test. *P* values of <0.05 were considered statistically significant.

RESULTS

Generation of PHD3-deficient mice. Mice deficient in PHD3 were generated by standard homologous recombination procedures in ES cells. The PHD3 targeting strategy involved removing a genomic region encompassing the promoter and first exon, including the translational initiation site (Fig. 1A and B), and cells from *PHD3*$^{-/-}$ homozygous animals expressed no PHD3 transcript (Fig. 1C and D, left panel) or protein (Fig. 1D, right panel). A small reduction in the expected number of *PHD3*$^{-/-}$ live births was noted among the offspring of heterozygous matings (*PHD3*$^{+/+}$, 77 [29%], *PHD3*$^{+/-}$, 145 [54%], *PHD3*$^{-/-}$, 47 [17%]), but otherwise *PHD3*$^{-/-}$ mice appeared healthy and reached adult life without obvious abnormality.

Enhanced survival of sympathetic neurons from PHD3$^{-/-}$ mice in vitro. Because experimental manipulation of PHD3 expression in cultured sympathetic neurons and PC12 cells has been reported to affect cell survival (23–25, 40), we directly compared the survival of sympathetic neurons obtained from the SCG of wild-type and *PHD3*$^{-/-}$ mice. Heterozygous mice were mated to obtain offspring of all three genotypes, and dissociated low-density cultures of SCG neurons were established from newborn littermates. To minimize variability arising from technical considerations, in this and all subsequent experiments, comparisons of ganglia explanted from mice of different genotypes were performed in a pair-wise fashion at the same experimental session. The neurons were cultured with a range of NGF concentrations, and neuronal survival was estimated 24 h after plating. At nonsaturating concentrations of NGF, the survival of neurons from *PHD3*$^{-/-}$ mice was consistently enhanced compared to that of neurons from wild-type mice (Fig. 2A, left panel). Interestingly, loss of PHD3 did not confer a survival advantage at very low NGF concentrations, suggesting that, although PHD3 reduces the capacity of neurons to survive in the presence of NGF, it is not required for the death of NGF-deprived neurons.

To test whether other prolyl hydroxylases that regulate HIF also affect the NGF survival response, similar cultures of SCG neurons were established from *PHD1*$^{-/-}$ and *PHD2*$^{+/-}$ mice (2) and compared with those from their littermate controls (*PHD2*$^{-/-}$ mice could not be used because they die in utero between embryonic day 12.5 [E12.5] and E14.5 [2, 41]). In contrast with neurons from *PHD3*$^{-/-}$ mice, no differences in NGF dose responses were observed (Fig. 2A, middle and right panels).

NGF promotes neuronal survival by binding to and activating the receptor tyrosine kinase TrkA (10). Because NT-3 is also capable of promoting the survival of neonatal SCG neurons in culture by a TrkA-dependent mechanism (12), we investigated whether inactivation of PHD3 affects the survival response of SCG neurons to this neurotrophin. As with NGF, SCG neurons from *PHD3*$^{-/-}$ mice survived more effectively with NT-3 than neurons from wild-type littermates (Fig. 2B).

In addition to sympathetic neurons, large numbers of sensory neurons in the developing peripheral nervous system are also dependent on NGF for survival. To ascertain whether the absence of PHD3 also affects the NGF survival response of these neurons, we established low-density dissociated cultures from two populations of sensory neurons that are mostly comprised of NGF-dependent neurons: those of the DRG and TG. In contrast to SCG neurons, the NGF dose responses of DRG and TG neurons from wild-type and *PHD3*$^{-/-}$ mice were completely overlapping (Fig. 2C). Since NGF withdrawal has been reported to induce PHD3 mRNA expression in sympathetic neurons (24), we considered whether this property might underlie the specificity of PHD3-dependent survival effects. To investigate this, we cultured SCG, DRG, and TG neurons with NGF and deprived them of this neurotrophin by extensive washing 12 h after plating. Measurement of PHD3 mRNA by

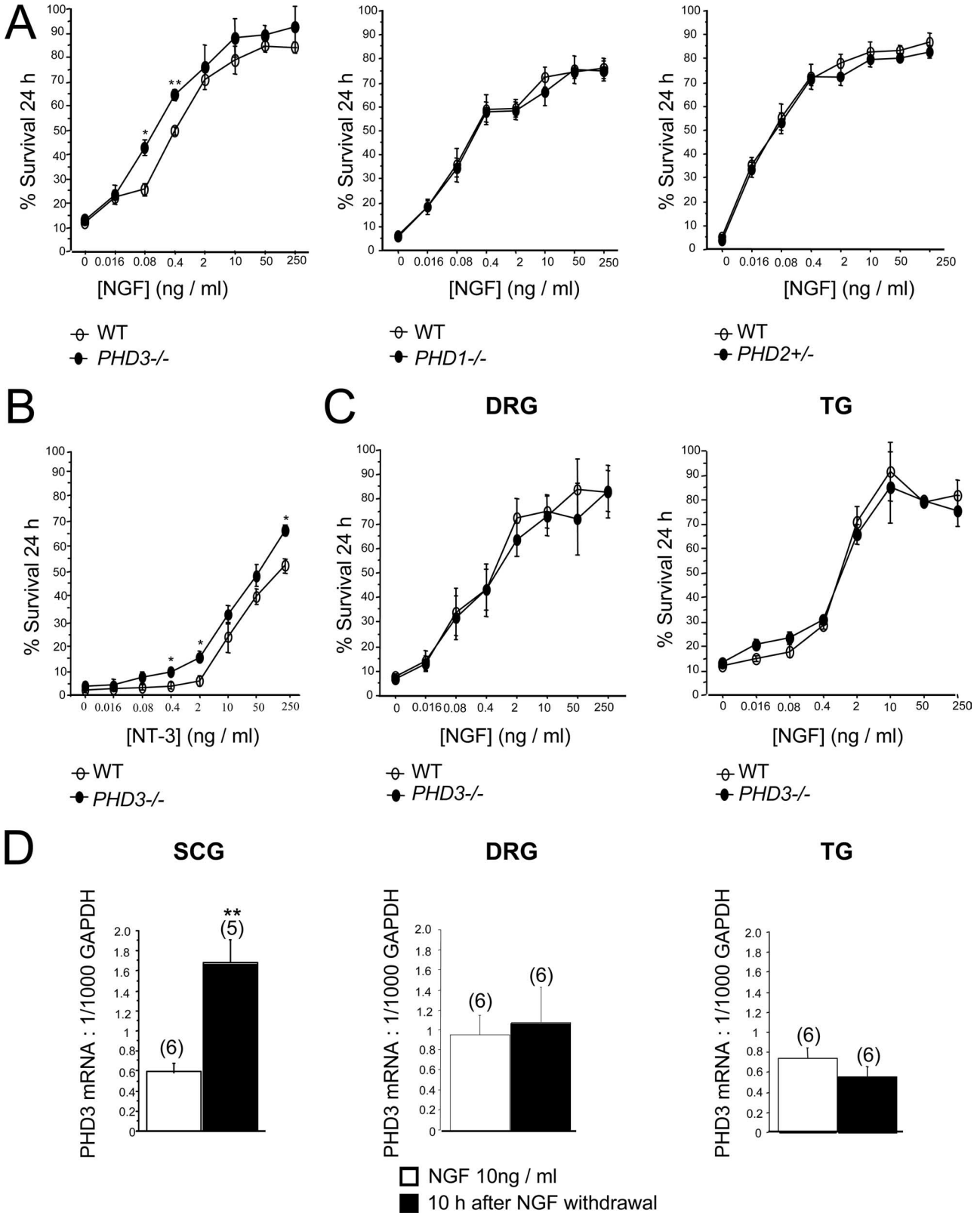

FIG. 2. Survival of neurons cultured from *PHD3*$^{-/-}$ mice. (A) NGF dose-response curves, demonstrating increased neuronal survival in neurons cultured from the SCG of P0 *PHD3*$^{-/-}$ mice but not *PHD1*$^{-/-}$ or *PHD2*$^{+/-}$ mice. Neuronal survival was estimated by expressing the number of surviving neurons after 24 h in culture as a percentage of the initial number of neurons at 3 h postplating. (B) NT-3 dose-response curve, showing increased survival in neurons cultured from the SCG of P0 *PHD3*$^{-/-}$ mice. (C) NGF dose-response curves, showing no change in survival in neurons cultured from the DRG and TG of P0 *PHD3*$^{-/-}$ mice. (D) Quantitative RT-PCR showing induction of PHD3 mRNA after NGF withdrawal in the SCG, but not the DRG or TG, from P0 wild-type mice. Values for this and all subsequent figures are presented as means ± SEM ($n = 3$) for dose-response curves, or n as indicated in parentheses. *, $P < 0.05$ versus control; **, $P < 0.01$ versus control.

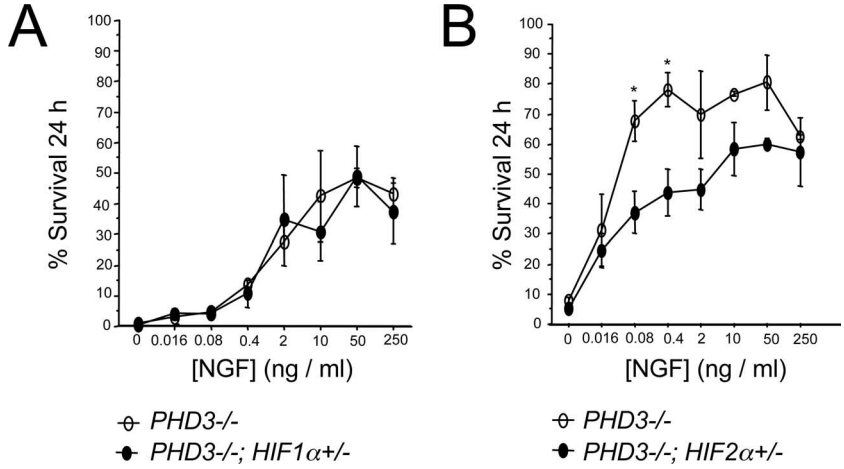

FIG. 3. HIF dependence of the PHD3 survival effect. NGF dose-response curves for neonatal SCG neurons showing no difference in survival of neurons derived from *PHD3*$^{-/-}$; *HIF-1*$\alpha^{+/-}$ versus *PHD3*$^{-/-}$ mice (A) and reduced survival of neurons derived from *PHD3*$^{-/-}$; *HIF-2*$\alpha^{+/-}$ versus *PHD3*$^{-/-}$ mice (B).

RT-PCR 10 h after deprivation revealed a greater-than-twofold increase in PHD3 mRNA relative to GAPDH mRNA in sympathetic neurons but no significant change in sensory neurons (Fig. 2D). Thus, both PHD3-dependent neuronal survival and responsiveness of PHD3 mRNA to NGF withdrawal appear to be specific to sympathetic neurons rather than a general property of NGF-sensitive neurons.

HIF-2-dependent survival in sympathetic neurons from *PHD3*$^{-/-}$ mice in vitro. Because of the known function of PHD3 as a HIF hydroxylase regulating the abundance of HIF-1α and HIF-2α, we investigated whether the influence of PHD3 on the NGF dose response of SCG neurons depends on either HIF-1α or HIF-2α. Since homozygous inactivation of HIF-1α or HIF-2α results in embryonic lethality (20, 33, 34, 42), we analyzed the effects of heterozygous inactivation by generating appropriate crosses with *PHD3*$^{-/-}$ animals to allow for littermate comparisons. Although we observed some variation in the overall survival of explanted neurons from *PHD3*$^{-/-}$ mice at different experimental sessions, clear differences were observed in pair-wise comparisons of *PHD3*$^{-/-}$ animals with and without heterozygous inactivation of different HIF-α isoforms. Heterozygous HIF-1α inactivation did not significantly affect the NGF dose response of cultured PHD3-deficient SCG neurons (*PHD3*$^{-/-}$ versus *PHD3*$^{-/-}$; *HIF-1*$\alpha^{+/-}$ littermate neonates) (Fig. 3A). In contrast, inactivating one allele of HIF-2α caused a significant shift in the NGF dose response of PHD3-deficient SCG neurons to higher NGF concentrations (*PHD3*$^{-/-}$ versus *PHD3*$^{-/-}$; *HIF-2*$\alpha^{+/-}$ littermate neonates) (Fig. 3B), suggesting that appropriate expression of HIF-2α, but not HIF-1α, is required for the influence of PHD3 on the NGF survival dose response in culture.

Enhanced NGF-promoted neurite growth of sympathetic neurons from *PHD3*$^{-/-}$ mice in vitro. In addition to supporting the survival of developing sympathetic neurons, NGF also promotes the growth of neurites from these neurons in culture (15). For this reason, we investigated neurite arbor size and complexity in sympathetic neurons from *PHD3*$^{-/-}$ mice. Low-density cultures of SCG neurons from P0 *PHD3*$^{-/-}$ and wild-type mice were grown with different concentrations of NGF, and neurite arbor size and complexity were quantified 24 h after plating. At subsaturating concentrations of NGF (Fig. 4B and C), but not at saturating levels (Fig. 4A), the neurite arbors of PHD3-deficient neurons were significantly longer than those of wild-type neurons. Sholl analysis, which provides a graphic representation of neurite branching with distance from the cell body, revealed that the neurite arbors of PHD3-deficient neurons were larger and more branched than those of wild-type mice in the presence of subsaturating levels of NGF (Fig. 4B and C). The typical appearance of the neurite arbors of PHD3-deficient and wild-type SCG neurons grown with subsaturating NGF are illustrated in Fig. 4D. Because the neurites in short-term SCG cultures, such as those used in our study, are exclusively axons rather than dendrites, we conclude that PHD3 also modulates axonal growth and branching in culture.

PHD3-deficient mice have increased numbers of SCG neurons. To ascertain the developmental and physiological relevance of our in vitro observations, we compared the number of neurons in the SCG of wild-type and *PHD3*$^{-/-}$ mice. The neuronal complement of the SCG of newborn animals was estimated by counting the number of neurons in trypsin-dissociated cell suspensions obtained from carefully dissected ganglia. In order to minimize variability assignable to genetic background, absolute age of neurons, and dissociation technique, these comparisons were made between ganglia explanted at the same experimental session from mice within the same litter. Neurons were recognized and distinguished from nonneuronal cells by their characteristic large, phase-bright, spherical cell bodies under phase-contrast optics. SCG dissected from *PHD3*$^{-/-}$ newborn mice appeared larger than those of wild-type littermates (Fig. 5A) and contained significantly more neurons (Fig. 5B). Likewise, stereological measurements carried out on serially sectioned SCG in 3- to 6-month-old mice revealed that the SCG was larger and contained significantly more neurons in *PHD3*$^{-/-}$ mice compared with age-matched wild-type animals (Fig. 5C). As expected, the number of neurons in the SCG of

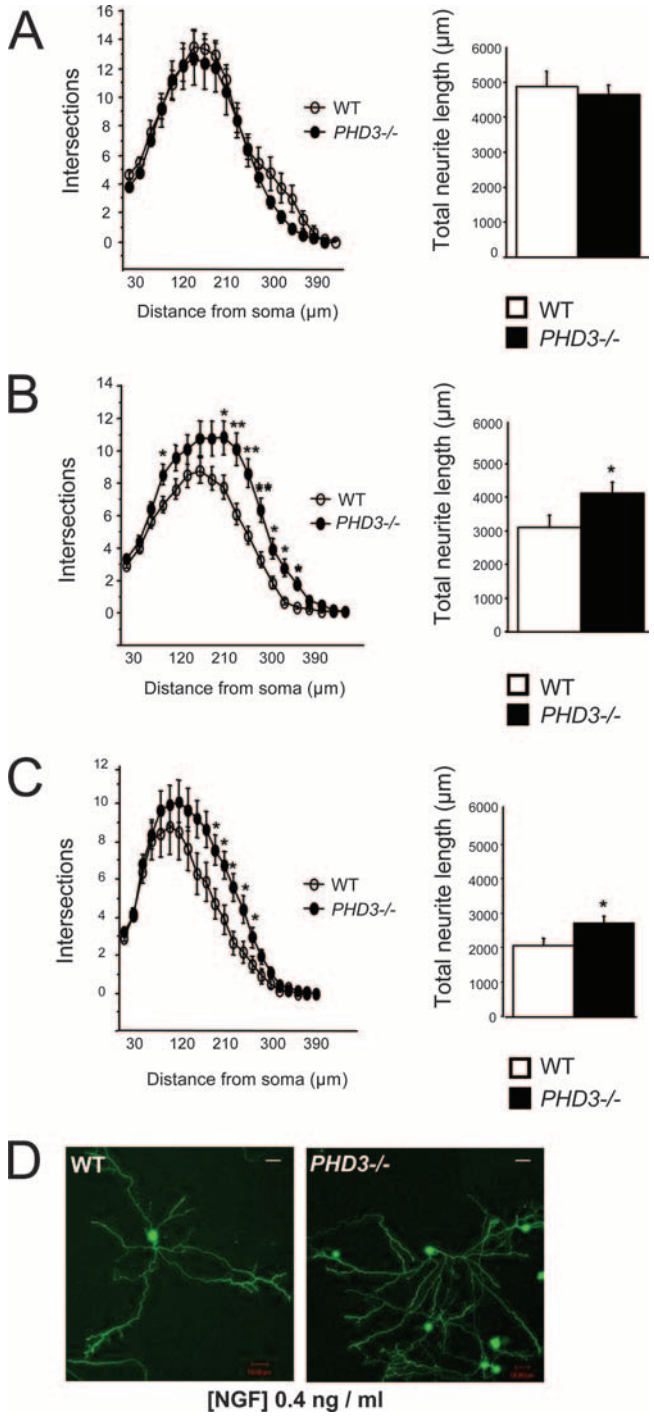

FIG. 4. Neurite length and arborization of sympathetic neurons cultured from *PHD3*$^{-/-}$ mice. Increased neurite length and arborization in P0 *PHD3*$^{-/-}$ mice at 0.4 (B) and 0.08 ng/ml NGF (C), but not at 10 ng/ml NGF (A). Neurite length is presented as the mean ± SEM on 40 to 70 neurons per genotype (similar results were obtained in three independent experiments). (D) Representative images of neurons cultured in 0.4 ng/ml NGF and fluorescently labeled with the vital dye calcein-AM. Bar, 50 μm.

wild-type adults was lower than that in newborns as a result of ongoing programmed cell death in the immediate postnatal period. However, the number of neurons in the SCG of *PHD3*$^{-/-}$ mice remained substantially unchanged between birth and adulthood, suggesting that programmed cell death during at least the postnatal period was largely curtailed in these mice. In keeping with this, we observed a modest reduction in the number of apoptotic or TUNEL-positive cells in the SCG from P0 *PHD3*$^{-/-}$ mice (~30% decrease, $n = 7$, $P < 0.05$, from 6.7×10^{-5} to 4.9×10^{-5} TUNEL-positive cells/μm^2 SCG area).

In contrast to the effect of *PHD3* deletion on SCG neuron number, there were no significant differences between the numbers of neurons in the SCG of either *PHD1*$^{-/-}$ or *PHD2*$^{+/-}$ neonates compared with wild-type littermates (data not shown).

To investigate the in vivo significance of HIF-α gene dosage on the survival of cultured neurons from *PHD3*$^{-/-}$ mice, we compared the number of neurons in the SCG of *PHD3*$^{-/-}$ versus *PHD3*$^{-/-}$; *HIF-1α*$^{+/-}$ littermate neonates and *PHD3*$^{-/-}$ versus *PHD3*$^{-/-}$; *HIF-2α*$^{+/-}$ littermate neonates. Consistent with the studies of survival in culture, these studies revealed that heterozygous inactivation of HIF-2α, but not HIF-1α, reduced the SCG neuronal population in *PHD3*$^{-/-}$ animals (Fig. 5D). Interestingly, this effect was not observed in the PHD3-positive background (comparison of wild-type versus *HIF-2α*$^{+/-}$ mice) (Fig. 5D). Further experiments designed to test the effect of PHD3 inactivation in the context of HIF-2α heterozygosity (comparison of *PHD3*$^{-/-}$; *HIF-2α*$^{+/-}$ versus *HIF-2α*$^{+/-}$ mice) revealed no significant differences in SCG cell numbers (Fig. 5D), suggesting that PHD3-dependent effects on cell number were affected by integrity of the HIF-2α pathway and vice versa. Taken together with our in vitro survival data, these in vivo observations suggest that the selective increase in SCG neurons in *PHD3*$^{-/-}$ mice results from reduced cell loss during the phase of programmed cell death in the perinatal period as a consequence of the enhanced sensitivity of PHD3-deficient neurons to NGF and that this effect is at least partially dependent on HIF-2α.

PHD3-deficient mice have increased numbers of cells in the adrenal medulla and carotid body. NGF-dependent cells of the sympathoadrenal axis extend to the neural crest-derived chromaffin and glomus cells of the adrenal medulla and carotid body. Our findings that *PHD3*$^{-/-}$ mice have significantly more sympathetic neurons than wild-type mice prompted us to examine cell number elsewhere in the sympathoadrenal system. Stereological analysis of adult mice (3 to 6 months old) revealed significantly more TH-positive cells in both the adrenal medulla and the carotid body (Fig. 6). Interestingly, though total numbers of cells were increased in both organs in *PHD3*$^{-/-}$ mice, overall organ volume was increased for the carotid body, but decreased for the adrenal medulla, in *PHD3*$^{-/-}$ mice (Fig. 6). The latter phenomenon may be explained by a reduction in chromaffin cell volume (from 1,743 μm^3 in wild-type to 1,195 μm^3 in *PHD3*$^{-/-}$ mice; $P < 0.05$; $n = 7$), consistent with the significant increase in TH-positive cell density in the adrenal medulla (Fig. 6A).

Sympathetic innervation of target tissues. Given that inactivation of PHD3 in vivo results in increased numbers of SCG neurons surviving to adulthood and that NGF is more effective in promoting neurite growth from cultured PHD3-deficient SCG neurons, we asked whether sympathetic innervation density is increased in *PHD3*$^{-/-}$ mice. The SCG innervates several anatomically discrete structures, including the iris, submandib-

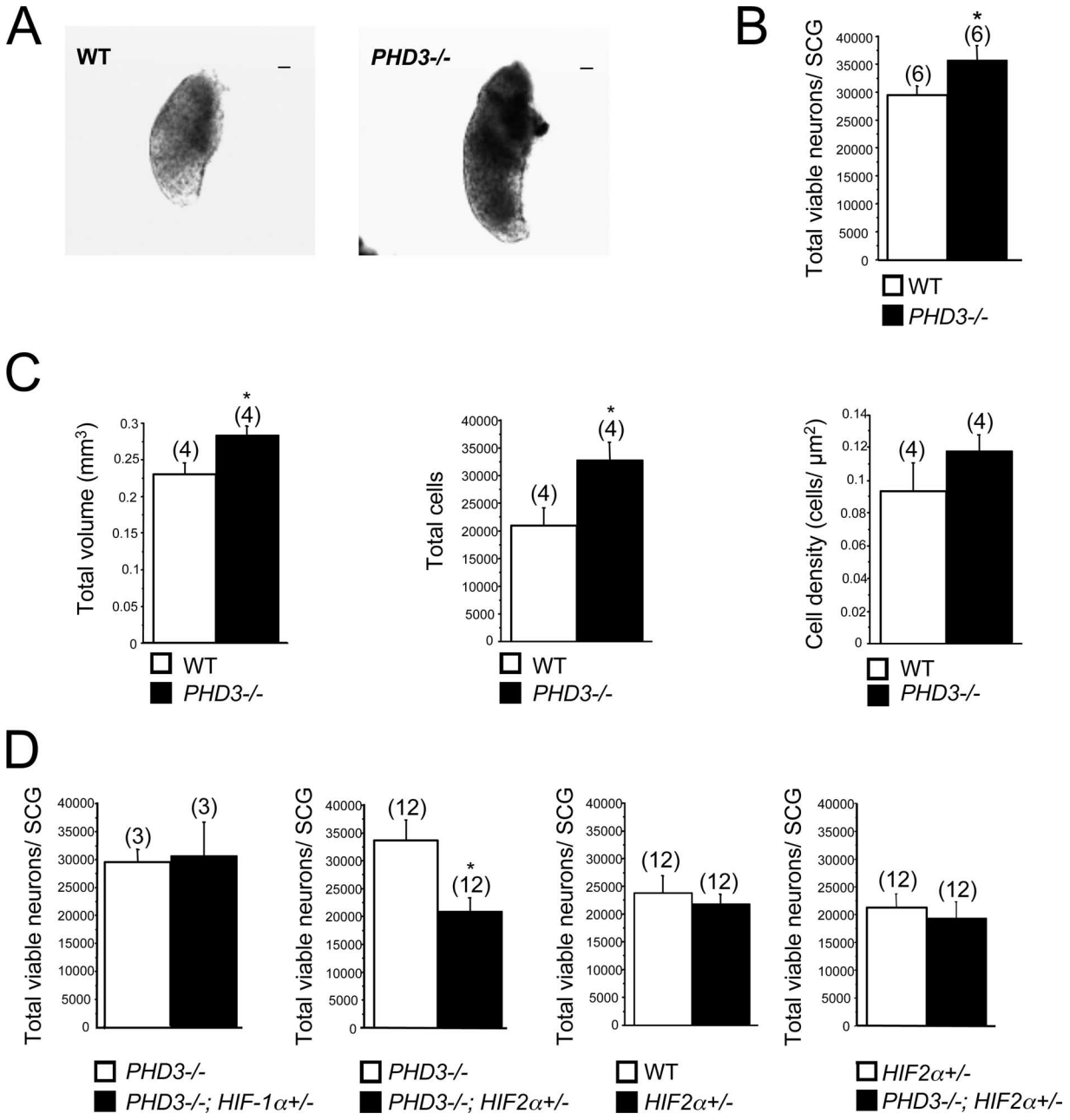

FIG. 5. Effect of genetic inactivation of PHD3 on anatomy of SCG. (A) Bright-field images of wild-type and *PHD3*$^{-/-}$ neonatal SCG. Bar, 100 μm. (B) Neuronal complement of neonatal SCG in wild-type and *PHD3*$^{-/-}$ mice; counts are of viable trypsin-dissociated neurons. (C) Stereological analysis of TH-positive neurons showing increased cell numbers in the SCG from adult *PHD3*$^{-/-}$ mice. (D) Comparison of neuronal complement of neonatal SCG in mice of the indicated genotypes. Counts are as for panel B. HIF-2α heterozygosity, but not HIF-1α heterozygosity, is associated with reduced neuronal complement.

ular gland, and pineal gland, whose innervation density can be relatively easily estimated by quantifying the area occupied by TH-positive nerve fibers in tissue sections. Surprisingly, this analysis revealed significantly fewer TH-positive fibers in the iris, submandibular gland, and pineal gland of *PHD3*$^{-/-}$ mice compared with wild-type animals (Fig. 7A, B, and C).

Physiological effects on the sympathetic nervous system. We next sought to assess the integrity of physiological responses that are dependent on the sympathetic nervous system. Because of the reduced sympathetic innervation of the iris in *PHD3*$^{-/-}$ mice (Fig. 7A), we tested light-to-dark pupillary responses. While no differences in pupil diameter were seen under normal lighting conditions (150 lx) (Fig. 7D), pupil diameter was significantly decreased in the dark-adapted eye from *PHD3*$^{-/-}$ mice (0 lx) (Fig. 7D). This implies decreased tone in the sympathetically innervated dilator pupillae muscle fibers of *PHD3*$^{-/-}$ mice.

Since one of the most important roles of sympathoadrenal

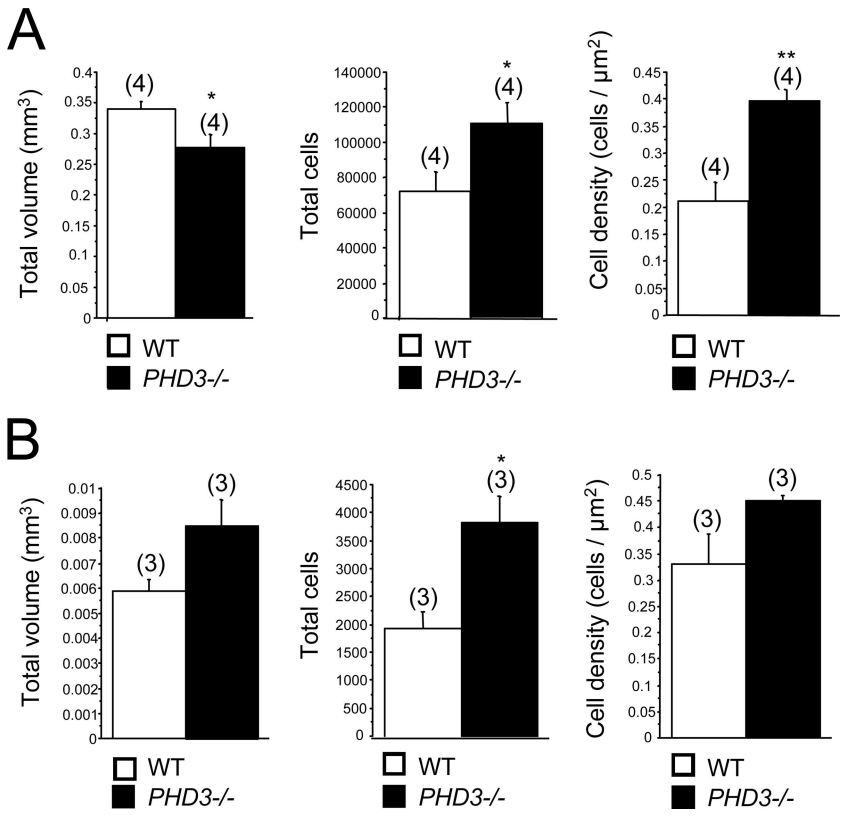

FIG. 6. Effect of genetic inactivation of PHD3 on the anatomy of other sympathoadrenal tissues, the adrenal medulla (A) and carotid body (B). Stereological analysis of TH-positive neurosecretory cells demonstrating increased cell numbers in the adrenal medulla (A) and carotid body (B) of adult *PHD3*$^{-/-}$ mice.

function is in the control of blood pressure, we went on to perform a series of measurements of systemic blood pressure regulation. First, a series of resting measurements were performed under anesthesia. These revealed a modest but significant reduction in blood pressure in *PHD3*$^{-/-}$ mice versus wild-type littermates (Table 1) but no significant differences in heart rate (Table 1). Consistent with reduced arterial pressure, we found that left ventricular weights were significantly reduced in *PHD3*$^{-/-}$ mice versus wild-type mice (Table 1).

To pursue the differences in blood pressure further, measurements of aortic blood pressure were repeated in conscious mice using radiotelemetry. These confirmed that, at rest, *PHD3*$^{-/-}$ mice were hypotensive compared to wild-type mice, with reduced systolic blood pressures (Fig. 8). Furthermore, the difference in systolic blood pressure was enhanced when the mice became active, with as much as 20 mm Hg difference in systolic pressure between *PHD3*$^{-/-}$ mice and littermate controls (Fig. 8).

If reduced blood pressure were due to sympathoadrenal dysfunction rather than a primary cardiac or vascular defect, we argued that responses to exogenous adrenoreceptor agonists should be preserved or even exaggerated. Under anesthesia, we measured responses to infusions of the α_1-agonist phenylephrine and the β_1-agonist dobutamine. Results are shown in Table 1. In response to the exogenous α_1-adrenoreceptor agonist phenylephrine, the maximal rise in blood pressure was exaggerated in *PHD3*$^{-/-}$ mice versus wild-type littermates. Interestingly, reflex bradycardia was blunted in *PHD3*$^{-/-}$ animals, suggesting that baroreceptor reflex sensitivity, a measure of endogenous autonomic function, was reduced. In response to the exogenous β_1-adrenoreceptor agonist dobutamine, *PHD3*$^{-/-}$ mice also showed an exaggerated increase in heart rate and contractility, consistent with reduced intrinsic sympathetic function rather than a primary cardiac or vascular cause of hypotension.

Finally, we tested adrenal medullary function both by measuring individual chromaffin cell catecholamine secretion rates by amperometry in explanted adrenal slices and by measuring total circulating catecholamine levels in intact animals. Amperometrically measured basal secretion of catecholamines was reduced by approximately 50% in chromaffin cells from *PHD3*$^{-/-}$ mice (Fig. 9A). Secretion in response to potassium-induced depolarization was similarly reduced (20 mM potassium) or reduced to a smaller extent (40 mM potassium) in *PHD3*$^{-/-}$ mice (Fig. 9A), consistent with reduced secretory capacity. Plasma catecholamine levels were also lower in *PHD3*$^{-/-}$ mice (Fig. 9B), suggesting that the observed increase in chromaffin cell number was not sufficient to compensate for the decrease in chromaffin cell functionality under physiological conditions.

DISCUSSION

Our findings show that the HIF prolyl hydroxylase PHD3 has an important role in regulating the development of the sympathoadrenal system and that its ablation has substantial physiological consequences that extend into adult life.

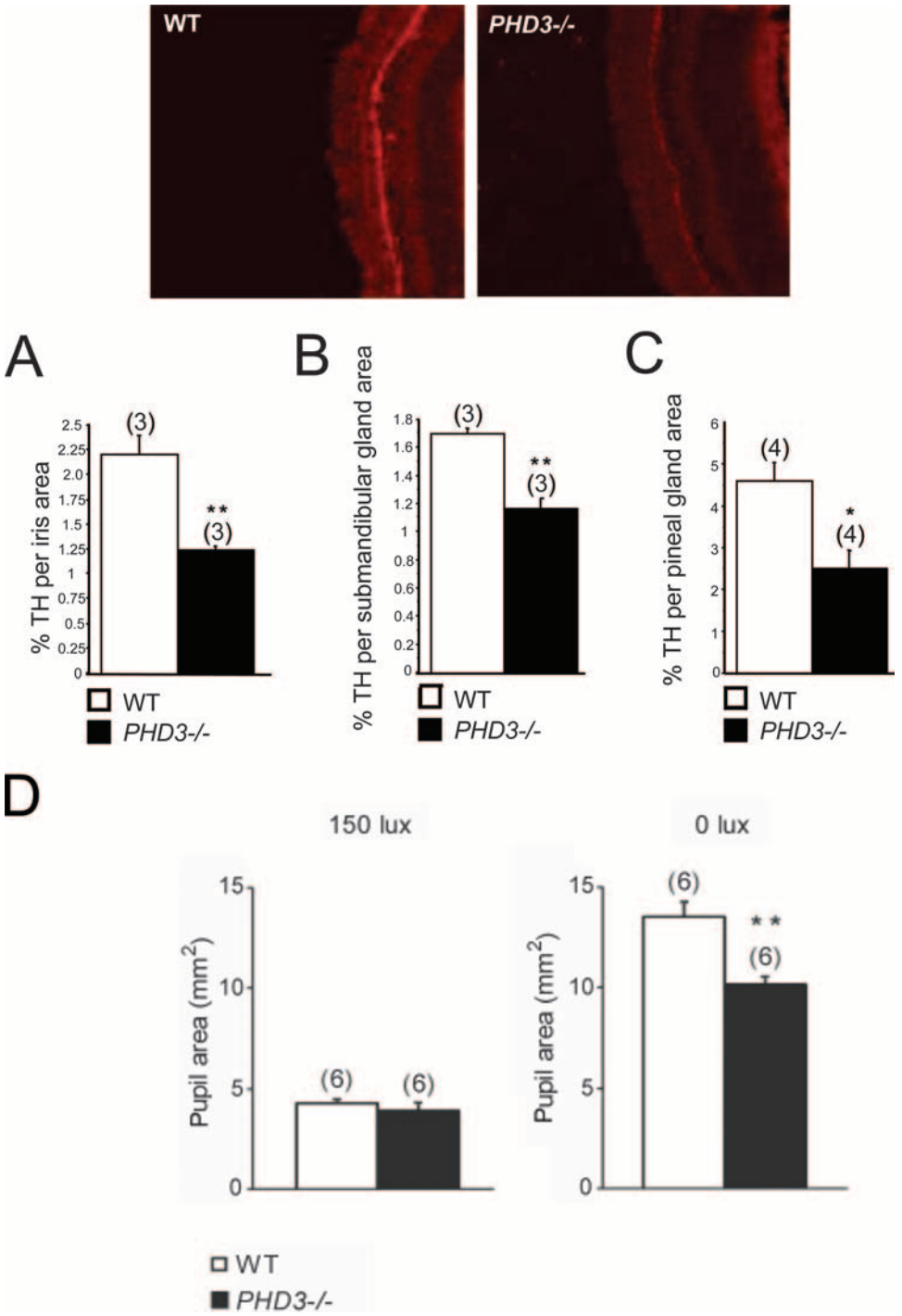

FIG. 7. Sympathetic innervation of SCG target tissues from *PHD3*$^{-/-}$ mice: immunohistochemistry demonstrating TH-positive neurons in SCG target tissues. Shown are representative images of TH-stained (bright red) neurons in the iris. Measured as the ratio of the TH-positively stained area over the total area of the SCG target tissue, there was decreased sympathetic innervation density of the iris (A), submandibular gland (B), and pineal gland (C). (D) Average pupil sizes in conscious, adult *PHD3*$^{-/-}$ mice and wild-type controls under normal illumination (150 lx of bright white light) and after 1 h of dark adaptation (0 lx).

We observed significantly more neurons in the SCG of newborn *PHD3*$^{-/-}$ mice compared with wild-type littermates, and this elevated number of SCG neurons was maintained to adulthood. The apparent failure of the neuronal complement of the SCG to decrease in *PHD3*$^{-/-}$ mice postnatally, when naturally occurring programmed cell death ordinarily matches the number of sympathetic neurons to the requirements of their targets, suggests that the elevated number of neurons in the SCG of PHD3-deficient mice is due to reduced cell death, in keeping with the observed shift in the NGF survival dose response

TABLE 1. Cardiovascular function in anesthetized mice[a]

Parameter (no. of animals in exptl groups)	Result for group		*P* value
	Wild type	*PHD3*$^{-/-}$	
Postmortem ventricular wt (10 WT, 7 *PHD3*$^{-/-}$)			
LV/body wt (mg/g)	3.19 ± 0.10	2.72 ± 0.06	0.001
RV/body wt (mg/g)	0.98 ± 0.04	0.99 ± 0.03	0.85
Arterial pressure (10 WT, 8 *PHD3*$^{-/-}$)			
Systolic (mmHg)	105 ± 3	94 ± 5	0.009
Diastolic (mmHg)	75 ± 2	69 ± 2	0.06
MAP (mm Hg)	89 ± 2	79 ± 1	0.005
LV hemodynamics: baseline (10 WT, 7 *PHD3*$^{-/-}$)			
dP/dt_{max} (mm Hg/s)	7,858 ± 474	7,363 ± 623	0.53
Heart rate (bpm)	437 ± 11	446 ± 17	0.66
LV hemodynamics: dobutamine (9 WT, 7 *PHD3*$^{-/-}$)			
dP/dt_{max} (% of baseline)	126 ± 4	152 ± 13	0.04
Heart rate (% of baseline)	117 ± 2	129 ± 3	0.006
LV hemodynamics: phenylephrine (5 WT, 4 *PHD3*$^{-/-}$)			
MAP (% of baseline)	135 ± 5	159 ± 22	0.07
Heart rate (% of baseline)	−31 ± 5	−21 ± 15	0.28
Baroreceptor gain (bpm/mm Hg)	−6.6 ± 1.3	−2.5 ± 0.9	0.04

[a] All values are means ± SEM. WT, wild type; MAP, mean arterial pressure; bpm, beats per minute.

of PHD3-deficient SCG neurons in culture to lower NGF concentrations. Interestingly, the effect of PHD3 inactivation on NGF responsiveness in the peripheral nervous system appears to be restricted to neurons of the sympathetic lineage, as neural crest-derived, NGF-dependent sensory neurons from *PHD3*$^{-/-}$ mice responded normally to NGF. It is unclear whether dysregulated apoptosis might occur in regions within the central nervous system in *PHD3*$^{-/-}$ mice. However, these mice are viable as adults, without obvious neurological abnormalities. In addition, brains from *PHD3*$^{-/-}$ mice were not obviously abnormal and were not significantly different in weight (0.43 ± 0.01 g versus 0.43 ± 0.00 g in *PHD3*$^{-/-}$ and wild-type males; 0.42 ± 0.01 g versus 0.44 ± 0.01 g in *PHD3*$^{-/-}$ and wild-type females). Nevertheless, these observations do not preclude dysregulation of apoptosis that is compensated for or might be revealed in pathological situations.

As well as enhancing the sensitivity of SCG neurons to the survival-promoting effects of NGF, deletion of PHD3 also makes these neurons more responsive to the neurite growth-promoting effects of NGF in culture. Because target-derived NGF is not only required for sympathetic neuron survival during development in vivo but is also responsible for the terminal growth and branching of sympathetic axons in their targets, we expected to find increased sympathetic innervation density in *PHD3*$^{-/-}$ mice. Surprisingly, we observed the opposite in several SCG target tissues in these animals. One possible explanation for this apparent paradox is that the increased number of sympathetic neurons innervating target tissues results in elevated uptake and removal of NGF from these tissues by retrograde axonal transport, resulting in lower ambient levels of NGF in the targets. Whereas retrograde transport of NGF in signaling endosomes to the cell bodies of sympathetic neurons is required for survival, the extent of axonal growth and branching in target tissues is governed by the ambient level of NGF in these tissues (15).

In addition to possessing elevated numbers of sympathetic neurons, *PHD3*$^{-/-}$ mice have increased numbers of chromaffin and glomus cells in the adrenal medulla and carotid body. Together with sympathetic neurons, these cells are derived from the sympathoadrenal neural crest lineage (22). Whether the increase in chromaffin or glomus cell number in *PHD3*$^{-/-}$ mice results from enhanced survival or from enhanced proliferation and/or differentiation of their precursors is not known.

Despite the increased number of cells in parts of the sympathoadrenal system of *PHD3*$^{-/-}$ mice, we observed impaired homeostatic and physiological responses regulated by this system, including reduced blood pressure, impaired light-to-dark pupillary dilation, and reduced catecholamine secretion from adrenal chromaffin cells, with lower plasma catecholamine levels in *PHD3*$^{-/-}$ mice. Sympathetic function is a key determinant of systemic blood pressure regulation (reviewed in reference 17), and elevated sympathetic activity is present in many forms of human hypertension. Apart from the findings reported here, we have not so far observed other basal abnormalities in *PHD3*$^{-/-}$ mice. Thus, though PHD3 could have other, as-yet-unknown effects on blood pressure regulation, the evidence for sympathetic hypofunction, reduced catecholamine secretion, reduced responses to activity, and preserved responses to exogenous adreno-agonists all support a causal link between sympathoadrenal dysregulation and blood pressure dysregulation in *PHD3*$^{-/-}$ animals.

Though previous cellular studies have implicated oxygen-dependent catalytic activity of PHD3 in the regulation of neuronal survival, these studies have given conflicting data on the role played by the known substrates HIF-1α and HIF-2α (23, 44). In the current work we found that heterozygous inactivation of HIF-2α, but not HIF-1α, had major effects on sympathetic neuronal survival and the neuronal complement of the SCG.

Interestingly, neonatal sympathetic failure has been ob-

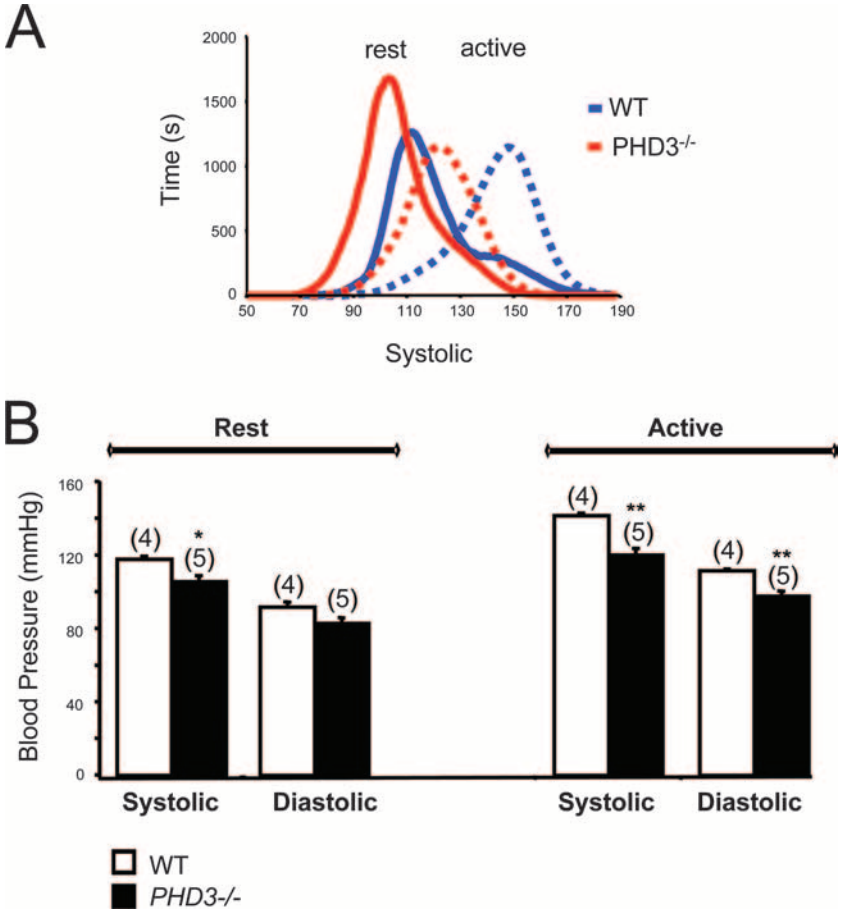

FIG. 8. Aortic blood pressures in conscious, adult *PHD3*$^{-/-}$ mice, as measured by radiotelemetry. (A) Pooled frequency histogram of systolic blood pressure over the 3-day recording period (using 1 mm Hg bins) from four (wild-type) or five (*PHD3*$^{-/-}$) resting (solid lines) and active (dotted lines) mice. (B) Average blood pressure recordings over a 3-day recording period. Decreased systolic and diastolic blood pressures were observed in *PHD3*$^{-/-}$ mice. These differences were enhanced when the mice were active.

served in *HIF-2α*$^{-/-}$ mice, and HIF-2α mRNA has been reported to be strongly expressed in sympathoadrenal tissues of the mouse (42). Though difficulties in obtaining background-free immunohistochemical signals precluded assessment in the mouse, we have also found that PHD3 is strongly expressed in the rat sympathoadrenal system, suggesting that the two proteins are coexpressed in this lineage (B. Wijeyekoon and C. W. Pugh, unpublished data). Interestingly, studies of small interfering RNA-mediated suppression of PHDs in tissue culture have indicated that PHD3 appears to exert greater regulatory effects on HIF-2α than HIF-1α (1). Taken together, the simplest synthesis of these findings is that PHD3 inactivation promotes sympathoadrenal neuronal survival, at least in part, through upregulation of HIF-2α. Nevertheless, consistent with a recent report of pharmacological PHD inhibition in sympathetic neurons (26), HIF-2α protein levels in the SCG of these normoxic animals were below the detection threshold for immunohistochemistry, so this could not be confirmed. It should also be noted that this explanation does not preclude the existence of other PHD3 substrates that may contribute to the observed effect. Indeed, the lack of effect of HIF-2α heterozygosity on a PHD3-positive background suggests that the relationship between HIF-2α and neuronal survival is not simple and depends on PHD3 status, perhaps implying the existence of other substrates in addition to HIF-2α. Thus, the importance of PHD3, as opposed to PHD1 or PHD2, in neuronal apoptosis might reflect the existence of a discrete, non-HIF, PHD3 substrate in this process, or the relative abundance of PHD3 in these cells coupled to the preferred targeting of HIF-2α by PHD3, or both.

Whether and how adult sympathetic hypofunction in *PHD3*$^{-/-}$ mice relates to dysregulation of HIF-2α is also unclear. Together with the finding of sympathetic failure in association with complete inactivation of HIF-2α in some but not all studies (33, 42), our findings suggest that although an intact PHD3/HIF-2α system is necessary for proper sympathoadrenal development, there is no simple relationship of hyper- or hypofunctionality to predicted effects of these genotypes on HIF-2α levels.

While we have demonstrated physiological deficits in adult *PHD3*$^{-/-}$ mice, it is not clear whether deficits arise purely as a consequence of PHD3 deficiency during development or whether there is an ongoing PHD3 requirement for sympathetic function in the adult. A great deal of interest has been generated by the possibility that environmental effects on development might influence medically important aspects of

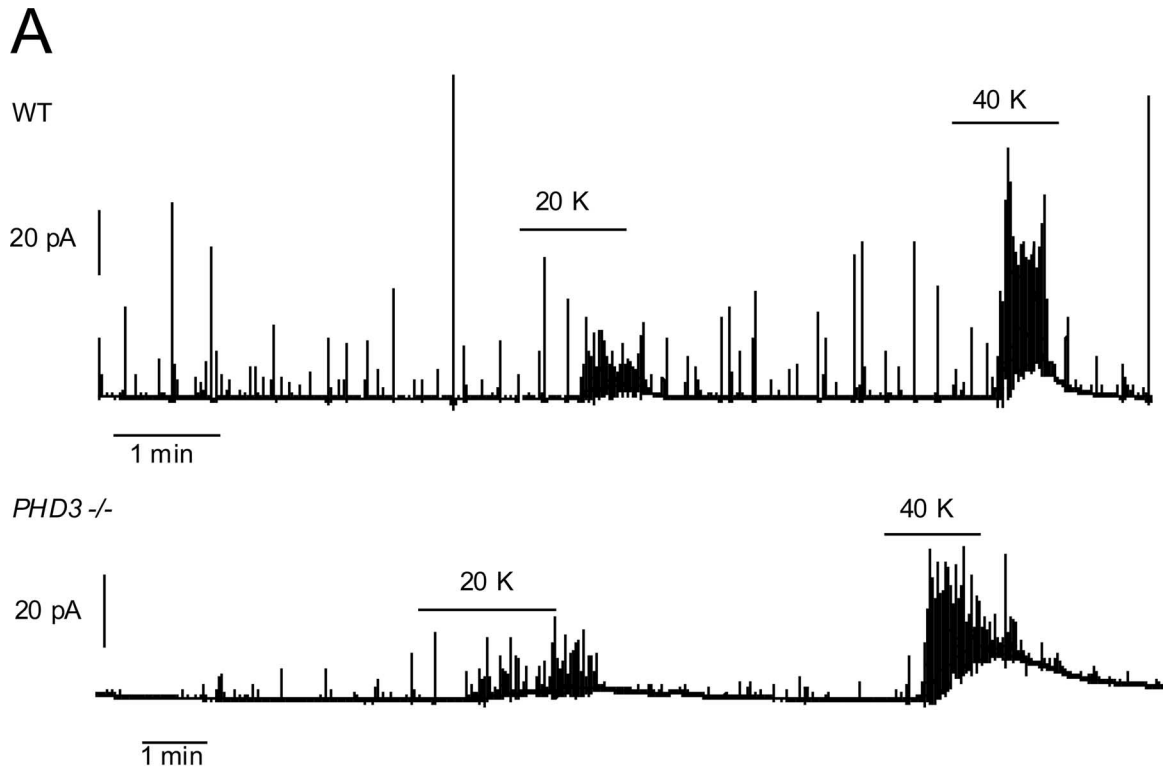

	Basal (fC / min)	20 K (fC/ s)	40 K (fC/ s)
WT	7477.9 ± 708.4 (5)	890.1 ± 62.1 (3)	3303.5 ± 348.5 (5)
PHD3-/-	4054.6 ± 629.2 (5)**	502.8 ± 95.5 (3)	2500.8 ± 346.2 (5)

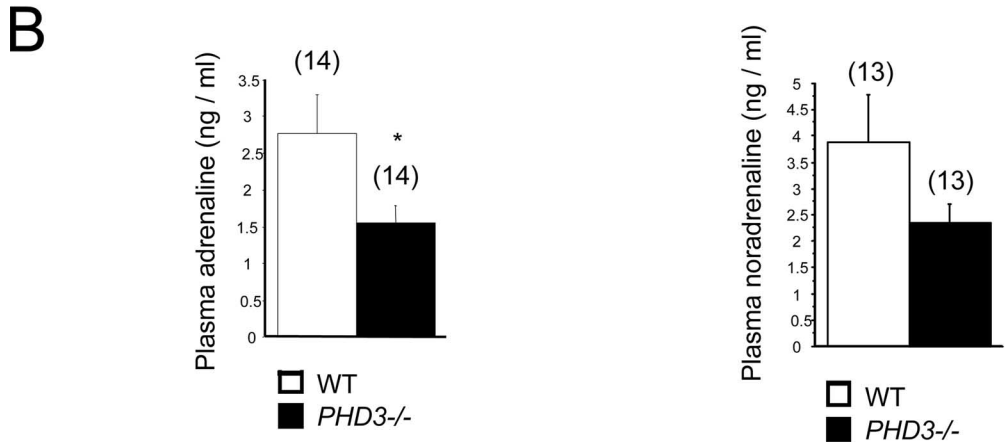

FIG. 9. Catecholamine secretion in *PHD3*$^{-/-}$ mice. (A) Representative amperometric recordings of basal catecholamine release, as well as responsiveness to induction by 20 mM and 40 mM potassium (20K and 40K), of adrenal slices isolated from adult mice. The table shows the secretion rate (in fC/min) under basal conditions, as well as with 20 mM and 40 mM potassium (20 and 40 K). (B) Circulating catecholamines (adrenaline and noradrenaline) from anesthetized, adult mice. Both adrenal slice and circulating catecholamines are reduced in *PHD3*$^{-/-}$ mice.

adult physiology, such as blood pressure regulation (reviewed in references 3 to 5 and 28). However, there are as yet few mechanistic clues as to how such processes might operate. The dependence of PHD activity on oxygen and cofactors, such as the Krebs cycle intermediate 2-oxoglutarate, Fe(II), and ascorbate (35), and inhibition of PHDs by metabolic intermediates, such as succinate, fumarate, pyruvate, and oxaloacetate (9, 18, 19, 21, 27, 36), raises the interesting possibility that environmental influences on PHD3 activity could perturb sympathetic development in a manner that might have important effects on cardiovascular control.

In conclusion, our findings reveal an important role for PHD3 in the developing sympathoadrenal system. It is an intriguing possibility that this connection between hypoxia pathways and the developing sympathoadrenal system might be a means by which changes in oxygen tension could influence key aspects of anatomical and physiological maturation of this system. Whether this provides a paradigm for environmental influences affecting development will be of interest in the future.

ACKNOWLEDGMENTS

This work was supported by the British Heart Foundation, the Wellcome Trust, and the EU Framework 6 Pulmotension Consortium.

We thank P. van Wesemael, M. Dewerchin, S. Wyns, E. Gils, B. Hermans, L. Kieckens, and L. Notebaert (Katholieke Universiteit Leuven, Belgium), as well as D. Adlam, S. Neubauer, R. Foster, and K. Buckler (University of Oxford, United Kingdom), for their contribution.

We have declared that no conflict of interest exists.

REFERENCES

1. **Appelhoff, R. J., Y. M. Tian, R. R. Raval, H. Turley, A. L. Harris, C. W. Pugh, P. J. Ratcliffe, and J. M. Gleadle.** 2004. Differential function of the prolyl hydroxylases PHD1, PHD2, and PHD3 in the regulation of hypoxia-inducible factor. J. Biol. Chem. **279:**38458–38465.
2. **Aragones, J., M. Schneider, K. Van Geyte, P. Fraisl, T. Dresselaers, M. Mazzone, R. Dirkx, S. Zacchigna, H. Lemieux, N. H. Jeoung, D. Lambrechts, T. Bishop, P. Lafuste, A. Diez-Juan, S. K. Harten, P. Van Noten, K. De Bock, C. Willam, M. Tjwa, A. Grosfeld, R. Navet, L. Moons, T. Vandendriessche, C. Deroose, B. Wijeyekoon, J. Nuyts, B. Jordan, R. Silasi-Mansat, F. Lupu, M. Dewerchin, C. Pugh, P. Salmon, L. Mortelmans, B. Gallez, F. Gorus, J. Buyse, F. Sluse, R. A. Harris, E. Gnaiger, P. Hespel, P. Van Hecke, F. Schuit, P. Van Veldhoven, P. Ratcliffe, M. Baes, P. Maxwell, and P. Carmeliet.** 2008. Deficiency or inhibition of oxygen sensor Phd1 induces hypoxia tolerance by reprogramming basal metabolism. Nat. Genet. **40:**170–180.
3. **Barker, D. J.** 1995. Fetal origins of coronary heart disease. BMJ **311:**171–174.
4. **Barker, D. J.** 2002. Fetal programming of coronary heart disease. Trends Endocrinol. Metab. **13:**364–368.
5. **Barker, D. J., S. P. Bagby, and M. A. Hanson.** 2006. Mechanisms of disease: in utero programming in the pathogenesis of hypertension. Nat. Clin. Pract. Nephrol. **2:**700–707.
6. **Bruick, R. K., and S. L. McKnight.** 2001. A conserved family of prolyl-4-hydroxylases that modify HIF. Science **294:**1337–1340.
7. **Butz, G. M., and R. L. Davisson.** 2001. Long-term telemetric measurement of cardiovascular parameters in awake mice: a physiological genomics tool. Physiol. Genomics **5:**89–97.
8. **Cavalieri, B.** 1966. Geometria degli indivisibili. Unione Tipografica Editrice, Torino, Italy.
9. **Dalgard, C. L., H. Lu, A. Mohyeldin, and A. Verma.** 2004. Endogenous 2-oxoacids differentially regulate expression of oxygen sensors. Biochem. J. **380:**419–424.
10. **Davies, A. M.** 2003. Regulation of neuronal survival and death by extracellular signals during development. EMBO J. **22:**2537–2545.
11. **Davies, A. M., K. F. Lee, and R. Jaenisch.** 1993. p75-deficient trigeminal sensory neurons have an altered response to NGF but not to other neurotrophins. Neuron **11:**565–574.
12. **Davies, A. M., L. Minichiello, and R. Klein.** 1995. Developmental changes in NT3 signalling via TrkA and TrkB in embryonic neurons. EMBO J. **14:**4482–4489.
13. **Epstein, A. C., J. M. Gleadle, L. A. McNeill, K. S. Hewitson, J. O'Rourke, D. R. Mole, M. Mukherji, E. Metzen, M. I. Wilson, A. Dhanda, Y. M. Tian, N. Masson, D. L. Hamilton, P. Jaakkola, R. Barstead, J. Hodgkin, P. H. Maxwell, C. W. Pugh, C. J. Schofield, and P. J. Ratcliffe.** 2001. C. elegans EGL-9 and mammalian homologs define a family of dioxygenases that regulate HIF by prolyl hydroxylation. Cell **107:**43–54.
14. **Garcia-Fernandez, M., R. Mejias, and J. Lopez-Barneo.** 2007. Developmental changes of chromaffin cell secretory response to hypoxia studied in thin adrenal slices. Pflugers Arch. **454:**93–100.
15. **Glebova, N. O., and D. D. Ginty.** 2005. Growth and survival signals controlling sympathetic nervous system development. Annu. Rev. Neurosci. **28:**191–222.
16. **Gordan, J. D., and M. C. Simon.** 2007. Hypoxia-inducible factors: central regulators of the tumor phenotype. Curr. Opin. Genet. Dev. **17:**71–77.
17. **Guyenet, P. G.** 2006. The sympathetic control of blood pressure. Nat. Rev. Neurosci. **7:**335–346.
18. **Hewitson, K. S., B. M. Lienard, M. A. McDonough, I. J. Clifton, D. Butler, A. S. Soares, N. J. Oldham, L. A. McNeill, and C. J. Schofield.** 2007. Structural and mechanistic studies on the inhibition of the hypoxia-inducible transcription factor hydroxylases by tricarboxylic acid cycle intermediates. J. Biol. Chem. **282:**3293–3301.
19. **Isaacs, J. S., Y. J. Jung, D. R. Mole, S. Lee, C. Torres-Cabala, Y. L. Chung, M. Merino, J. Trepel, B. Zbar, J. Toro, P. J. Ratcliffe, W. M. Linehan, and L. Neckers.** 2005. HIF overexpression correlates with biallelic loss of fumarate hydratase in renal cancer: novel role of fumarate in regulation of HIF stability. Cancer Cell **8:**143–153.
20. **Iyer, N. V., L. E. Kotch, F. Agani, S. W. Leung, E. Laughner, R. H. Wenger, M. Gassmann, J. D. Gearhart, A. M. Lawler, A. Y. Yu, and G. L. Semenza.** 1998. Cellular and developmental control of O2 homeostasis by hypoxia-inducible factor 1 alpha. Genes Dev. **12:**149–162.
21. **Koivunen, P., M. Hirsila, A. M. Remes, I. E. Hassinen, K. I. Kivirikko, and J. Myllyharju.** 2007. Inhibition of hypoxia-inducible factor (HIF) hydroxylases by citric acid cycle intermediates: possible links between cell metabolism and stabilization of HIF. J. Biol. Chem. **282:**4524–4532.
22. **Le Douarin, N. M.** 1986. Cell line segregation during peripheral nervous system ontogeny. Science **231:**1515–1522.
23. **Lee, S., E. Nakamura, H. Yang, W. Wei, M. S. Linggi, M. P. Sajan, R. V. Farese, R. S. Freeman, B. D. Carter, W. G. Kaelin, Jr., and S. Schlisio.** 2005. Neuronal apoptosis linked to EglN3 prolyl hydroxylase and familial pheochromocytoma genes: developmental culling and cancer. Cancer Cell **8:**155–167.
24. **Lipscomb, E. A., P. D. Sarmiere, R. J. Crowder, and R. S. Freeman.** 1999. Expression of the SM-20 gene promotes death in nerve growth factor-dependent sympathetic neurons. J. Neurochem. **73:**429–432.
25. **Lipscomb, E. A., P. D. Sarmiere, and R. S. Freeman.** 2001. SM-20 is a novel mitochondrial protein that causes caspase-dependent cell death in nerve growth factor-dependent neurons. J. Biol. Chem. **276:**5085–5092.
26. **Lomb, D. J., J. A. Straub, and R. S. Freeman.** 2007. Prolyl hydroxylase inhibitors delay neuronal cell death caused by trophic factor deprivation. J. Neurochem. **103:**1897–1906.
27. **Lu, H., C. L. Dalgard, A. Mohyeldin, T. McFate, A. S. Tait, and A. Verma.** 2005. Reversible inactivation of HIF-1 prolyl hydroxylases allows cell metabolism to control basal HIF-1. J. Biol. Chem. **280:**41928–41939.
28. **McMillen, I. C., and J. S. Robinson.** 2005. Developmental origins of the metabolic syndrome: prediction, plasticity, and programming. Physiol. Rev. **85:**571–633.
29. **Mills, P. A., D. A. Huetteman, B. P. Brockway, L. M. Zwiers, A. J. Gelsema, R. S. Schwartz, and K. Kramer.** 2000. A new method for measurement of blood pressure, heart rate, and activity in the mouse by radiotelemetry. J. Appl. Physiol. **88:**1537–1544.
30. **Niederhoffer, N., L. Hein, and K. Starke.** 2004. Modulation of the baroreceptor reflex by alpha 2A-adrenoceptors: a study in alpha 2A knockout mice. Br. J. Pharmacol. **141:**851–859.
31. **Oppenheim, R. W.** 1991. Cell death during development of the nervous system. Annu. Rev. Neurosci. **14:**453–501.
32. **Pardal, R., and J. Lopez-Barneo.** 2002. Carotid body thin slices: responses of glomus cells to hypoxia and K^+-channel blockers. Respir. Physiol. Neurobiol. **132:**69–79.
33. **Peng, J., L. Zhang, L. Drysdale, and G. H. Fong.** 2000. The transcription factor EPAS-1/hypoxia-inducible factor 2α plays an important role in vascular remodeling. Proc. Natl. Acad. Sci. USA **97:**8386–8391.
34. **Ryan, H. E., J. Lo, and R. S. Johnson.** 1998. HIF-1 alpha is required for solid tumor formation and embryonic vascularization. EMBO J. **17:**3005–3015.
35. **Schofield, C. J., and Z. Zhang.** 1999. Structural and mechanistic studies on 2-oxoglutarate-dependent oxygenases and related enzymes. Curr. Opin. Struct. Biol. **9:**722–731.
36. **Selak, M. A., S. M. Armour, E. D. MacKenzie, H. Boulahbel, D. G. Watson, K. D. Mansfield, Y. Pan, M. C. Simon, C. B. Thompson, and E. Gottlieb.** 2005. Succinate links TCA cycle dysfunction to oncogenesis by inhibiting HIF-alpha prolyl hydroxylase. Cancer Cell **7:**77–85.
37. **Semenza, G. L.** 2003. Targeting HIF-1 for cancer therapy. Nat. Rev. Cancer **3:**721–732.

38. **Sholl, D. A.** 1953. Dendritic organization in the neurons of the visual and motor cortices of the cat. J. Anat. **87:**387–406.
39. **Stalmans, I., Y. S. Ng, R. Rohan, M. Fruttiger, A. Bouche, A. Yuce, H. Fujisawa, B. Hermans, M. Shani, S. Jansen, D. Hicklin, D. J. Anderson, T. Gardiner, H. P. Hammes, L. Moons, M. Dewerchin, D. Collen, P. Carmeliet, and P. A. D'Amore.** 2002. Arteriolar and venular patterning in retinas of mice selectively expressing VEGF isoforms. J. Clin. Investig. **109:**327–336.
40. **Straub, J. A., E. A. Lipscomb, E. S. Yoshida, and R. S. Freeman.** 2003. Induction of SM-20 in PC12 cells leads to increased cytochrome *c* levels, accumulation of cytochrome *c* in the cytosol, and caspase-dependent cell death. J. Neurochem. **85:**318–328.
41. **Takeda, K., V. C. Ho, H. Takeda, L. J. Duan, A. Nagy, and G. H. Fong.** 2006. Placental but not heart defects are associated with elevated hypoxia-inducible factor alpha levels in mice lacking prolyl hydroxylase domain protein 2. Mol. Cell. Biol. **26:**8336–8346.
42. **Tian, H., R. E. Hammer, A. M. Matsumoto, D. W. Russell, and S. L. McKnight.** 1998. The hypoxia-responsive transcription factor EPAS1 is essential for catecholamine homeostasis and protection against heart failure during embryonic development. Genes Dev. **12:**3320–3324.
43. **West, M. J.** 1993. New stereological methods for counting neurons. Neurobiol. Aging **14:**275–285.
44. **Xie, L., R. S. Johnson, and R. S. Freeman.** 2005. Inhibition of NGF deprivation-induced death by low oxygen involves suppression of BIMEL and activation of HIF-1. J. Cell Biol. **168:**911–920.